

# Lecture 7

## Basic Principles of Climate

Raymond T. Pierrehumbert

### One-dimensional climate models

#### Introduction

In zero-dimensional models, variations of temperature with latitude cannot be taken into account. This is potentially problematic because there is a significant pole-equator temperature difference, and because the surface properties of the pole can differ remarkably from those of the equator (due largely to ice). As a next step up in sophistication for simple climate models, we therefore turn to one-dimensional models, in which the temperature  $T(\phi, t)$  depends both on latitude  $\phi$  and time  $t$ .

An important first ingredient is the input solar heating: The amount of solar radiation per unit area that is received at the top of the atmosphere varies with latitude and with the time of the year. This is given by the solar constant  $S_0$  (which is about  $1370 \text{ W m}^{-2}$ ) times a flux factor  $F(\phi, t)$  that gives the dependence on latitude and time, which is given in Fig. 1. There are two competing effects that determine this flux factor. First, the inclination of the surface relative to the incoming radiation gives greater weight to the regions where the sun is overhead (the tropics). This is offset by the second effect, that of the increase of the length of the day, which promotes solar heating at the poles in summer. For the present-day Earth's inclination, the effect of the day's length exceeds the inclination effect and as shown in figure 1, the polar region in the summer hemisphere receives more radiation than the equatorial region. Were it not for moderating influence of the ice, atmosphere and ocean, the hottest regions would therefore migrate from pole to pole through the year, and Antarctica would have the warmest summer on Earth.

Given that the climate moderates the annual variation of solar heating, the flux factor  $F(\phi, t)$  is not the most useful characterization of the energy input for a watery planet like Earth. Instead, we turn to the annual average, shown in Fig. 2, which has a minimum at the poles and a maximum at the equator, and varies by a factor of about two. Also shown is the annual average for an Earth with zero obliquity, for which the variation between pole and equator is much larger (because the day's length is constant and there is only the inclination effect).

Based on the annual average, one expects that, if there were no latitudinal heat transport, the atmosphere would be in local radiative equilibrium at every position and the

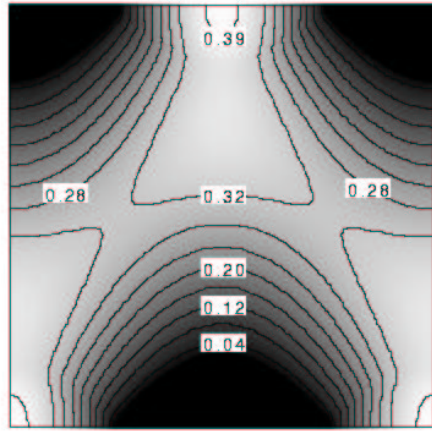


Figure 1: Flux factor  $F(\phi, t)$  as a function of time on the horizontal axis and latitude on the vertical axis. the time range is from January to December, the latitude axis from  $90^\circ S$  to  $90^\circ N$ .

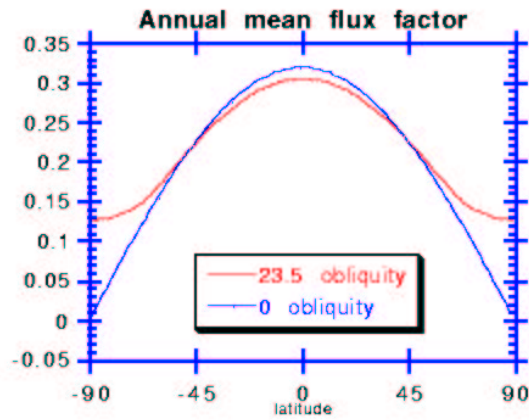


Figure 2: Annual mean flux factor as a function of latitude.

temperature difference between equator and pole would be very large. Because such a severe temperature drop is not observed, there must be a latitudinal transport of heat that reduces the variation. Satellite imagery of the actual energy budget at the top of the atmosphere (solar heating minus OLR) is shown in Fig. 3. The radiative imbalance is about  $75$  to  $100 \text{ Wm}^{-2}$  in the equatorial region, and about  $-100$  to  $-150 \text{ Wm}^{-2}$  at the poles. Also noticeable in the figure are the outlines of the continents (particularly South America) and the relatively light Sahara desert. The latter is a significant contributor to OLR due to the high cooling effect of sand, the dry atmosphere and because there are very few clouds. The

ice cover of Antarctica is also visible to the lower right.

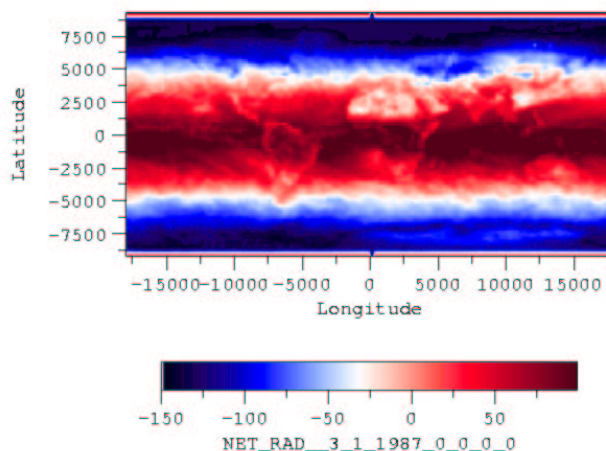


Figure 3: *Net energy budget in  $Wm^{-2}$  at the top of the atmosphere.*

The latitudinal heat transport occurs partly through the atmosphere and partly through the oceans. At  $45^{\circ}N$ , the atmosphere is responsible for most of the heat transport, except locally in the North Atlantic (in the Gulf Stream region). A large amount of the atmospheric heat transport occurs through latent heat transport, as water evaporates in the tropical region and precipitates at higher latitudes. In the oceans, the heat transport is accomplished through both the wind-driven and thermohaline circulation.

The latitudinal distribution of the energy budget at the top of the atmosphere is compared with the sea surface temperature (SST) in Fig. 4. The temperature is relatively constant between about  $20^{\circ}S$  and  $20^{\circ}N$ . A simple explanation for this flat temperature profile will be given later with the help of a conceptual model of tropical temperatures.

In addition to temperature, there is also a significant variation with latitude in the moisture content of the atmosphere; maps of monthly precipitation and specific humidity are shown in Figs. 5 and 6. Areas of large precipitation are found near the equator over the Intertropical Convergence Zone (the “ITCZ”), over the warm pool in the western Pacific ocean (labelled W) and above the storm tracks of the Atlantic and Pacific (labelled ST). There is also a significant amount over the rainforests of the Amazon basin and the Congo.

The specific humidity is high in a band between  $20^{\circ}S$  and the equator (Fig. 6) and there is a sharp gradient in relative humidity over the central Pacific. This latitudinal distribution of precipitation and specific humidity does not result from temperature variations, but can be understood from the mean circulation pattern of the atmosphere in the tropics, which is part of the low-latitude “Hadley Cell”: Directly above the surface, air converges to the equator, where it rises in a relatively narrow band (the ITCZ), then spreads out again to the north and south at higher altitudes to create a compensating subsidence flow of a much larger scale. Evaporation seeds the surface flow with water vapour which condenses over the ITCZ as the rising air cools, to produce a large amount of rainfall over that area.

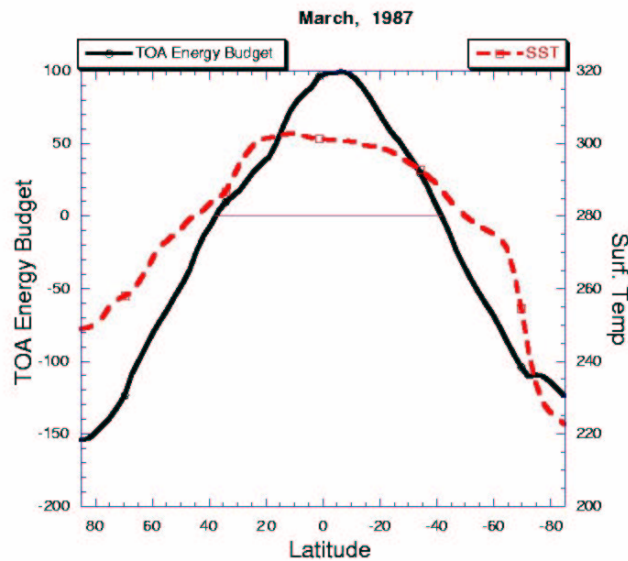


Figure 4: Net energy budget at the top of the atmosphere (TOA) and surface temperature averaged over March 1987 as a function of latitude.

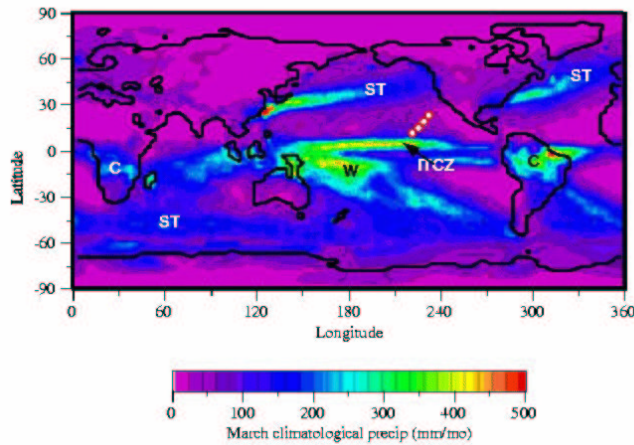


Figure 5: Climatological precipitation in March in mm/month.

The subsiding flow is much drier, and as it warms with descent, the relative humidity becomes even lower. Specific humidity is conserved as air subsides, and the air in the subsiding branch is dry because it is brought down from a cold, dry place. This action has the potential to create very strong humidity variations with latitude, variations that are, in fact, much stronger than those which are observed. The subsiding flow is wetter than this simple picture predicts because of latitudinal transport of moisture by turbulent

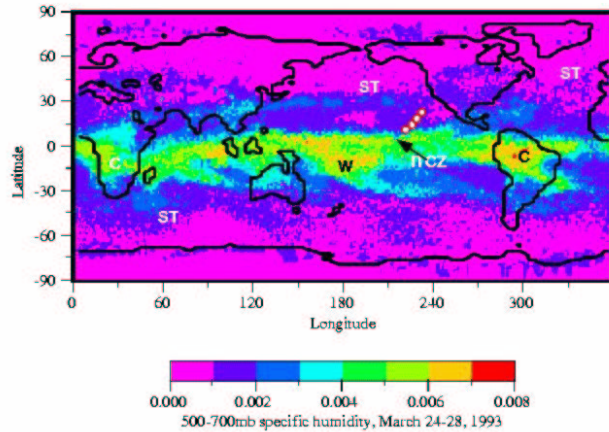


Figure 6: *Specific humidity of the 500-700 mb level, averaged over the period of March 24-28, 1993.*

eddies (the precise origin of these fluid motions is not completely understood, but possible candidates are tropical waves, baroclinic instability, westerly wind bursts and the “Madden-Julian Oscillation”). Although the subsidence region is still dry compared to the ITCZ, the increase in relative humidity due to the latitudinal eddy transport is important because of the logarithmic dependence of OLR on specific humidity. Dry as the subtropics are, it still matters precisely *how dry* they are.

The circulation of the Hadley cell is an essential element of the meridional heat transport. Between  $20^{\circ}S$  and  $20^{\circ}N$  the coriolis force is relatively weak and the circulation is dominated by the Hadley cell. In fact, the structure of the Hadley cell is more complicated than suggested above: The rising motions typically occur in the summer hemisphere, and the downward motions in the winter one. As a result, at a particular time, the circulation in the meridional-vertical plane is quite asymmetric, with rising air in one hemisphere and subsidence in the other. Moreover, during the year, the ITCZ moves only over a relatively short distance, whereas the subsidence region moves over a much greater distance. This makes the annually averaged Hadley circulation rather symmetric around the equator, in contrast to the instantaneous pattern.

From the perspective of energetics, the Hadley circulation is powered by two different mechanisms acting in the rising and subsiding parts of the flow. The rising flow is energized by sunlight, which through evaporation laces the upflow with water vapour (“liquid sunshine”); the vapour subsequently condenses to release latent heat on adiabatic cooling. The descending flow acts like a huge compressor, heating the air and generating upward infra-red radiation. Any imbalances between the two regions are rapidly communicated and equalized by pressure forces, which is why diffusive effects are secondary and strong water vapour gradients can be maintained. Overall, this relatively rapid pressure equalization sustains a fairly constant temperature throughout the tropics; the toy model described below illustrates these physical ideas.

## Tropical heat transport

Since the total energy reaching the earth's surface arrives primarily in the equatorial regions, it's important to understand the mechanisms of heat transport there. We formulate this problem in terms of a one-dimensional model, in which all longitudinal variation is neglected. The model is based on work by Held & Hou (1980) and Lindzen & Hou (1988, *JAS*, **24**, 151).

The basic equations we start with are the zonal and meridional shallow-water equations on the equatorial  $\beta$ -plane:

$$\begin{aligned}\partial_t U + U\partial_x U + V\partial_y U - \beta y V &= -\partial_x h \\ \partial_t V + U\partial_x V + V\partial_y V + \beta y U &= -\partial_y h\end{aligned}$$

where  $U$  and  $V$  are the zonal and meridional velocities respectively, and  $h$  is the depth of the atmosphere.

We consider relatively slow (linear), steady motions with no zonal structure, and so the shallow-water equations reduce to

$$\begin{cases} V\partial_y U - \beta y V = 0 \\ \beta y U = -\partial_y h \end{cases}$$

Note that, in the tropical regions of interest,  $f \approx 0$ . Because there is then no Coriolis term to balance the longitudinal pressure gradient, the usual geostrophic balance cannot be attained. Also, the mass below a surface of constant potential temperature is roughly proportional to the mean temperature of the layer. In the following we will therefore use  $h$  as a proxy for temperature  $T$  in order to determine the thermodynamic state of the atmosphere.

This model is a fairly good representation of the upper branch of the Hadley cell (the high-altitude flow), where we can reasonably neglect dissipative effects. The lower branch of the cell (the flow just above the surface), however, is controlled in part by stronger dissipation, which one might try to model by adding friction terms to the equations.

The  $x$ -momentum equation can be re-arranged to give

$$V\partial_y \left( U - \frac{1}{2}\beta y^2 \right) = 0, \tag{1}$$

so that

$$\left( U - \frac{1}{2}\beta y^2 \right) = \text{constant}. \tag{2}$$

This is essentially a statement of angular momentum conservation. If we consider a equatorially-symmetric Hadley circulation, then  $U = 0$  at  $y = 0$  and we have:

$$U = \frac{1}{2}\beta y^2. \tag{3}$$

Integrating the  $y$ -momentum equation over  $y$  now gives the following relation for the meridional profile of the height of the tropopause:

$$h = h_{eq} - \frac{1}{8}\beta^2 y^4, \tag{4}$$

which is plotted in Fig. , and roughly corresponds to the meridional temperature distribution. The flatness of the curve near the equator comes from the dependence of  $h$  on the fourth power of  $y$ .

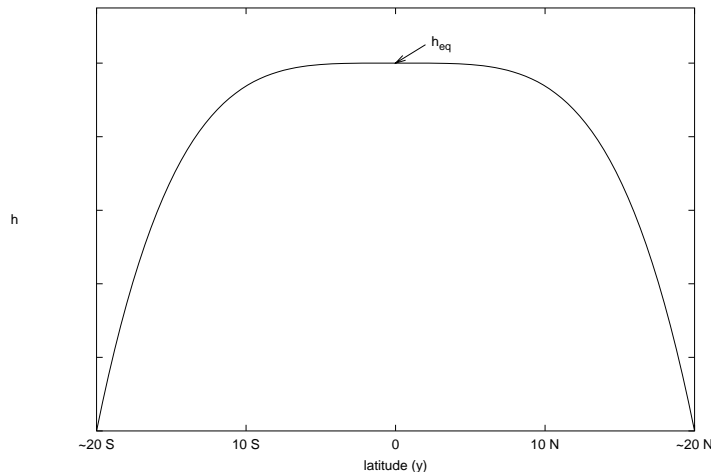


Figure 7: Layer depth (mean temperature) as a function of latitude

This profile is obtained with the assumption of zero zonal velocity,  $U$ , at the equator. On the other hand, we could have imposed the following, less restrictive, condition:  $U(y = 0) = U_{eq}$ , which case,

$$\frac{\partial h}{\partial y} = -\beta y \left( U_{eq} + \frac{1}{2} \beta y^2 \right) \quad (5)$$

and

$$h = -\frac{\beta^2 y^4}{8} - \frac{\beta y^2 U_{eq}}{2} + h_{eq}. \quad (6)$$

The quadratic term on the right-hand side of equation (6) may cause (for  $U_{eq} < 0$ ) a depression of the height of the tropopause at the equator (see figure 8).

At this stage we have not introduced the solar heat input, and so the symmetry properties of the temperature profile are independent of the details of the solar forcing. Also, we have no way of determining the latitudinal extent of the Hadley cell,  $[-y_{max}, y_{max}]$ . Given that the cell must continuously match onto a mid-latitude atmosphere in which we might wish to prescribe the depth  $h(y_{max}) = h_{mid}(y_{max})$  by the condition of radiative equilibrium (which determines the function  $h_{mid}(y_{max})$ ), this is equivalent to having an arbitrary equatorial depth,  $h_{eq}$ . The cell size and equatorial depth are, however, related by

$$h_{eq} = h_{mid} + \frac{1}{8} \beta y_{max}^4 + \frac{1}{2} \beta U_{eq} y_{max}^2. \quad (7)$$

To complete the solution, we evaluate the global atmospheric meridional mass flux:

$$\frac{\partial}{\partial y} (Vh) = -\frac{h}{\tau} + Q, \quad (8)$$

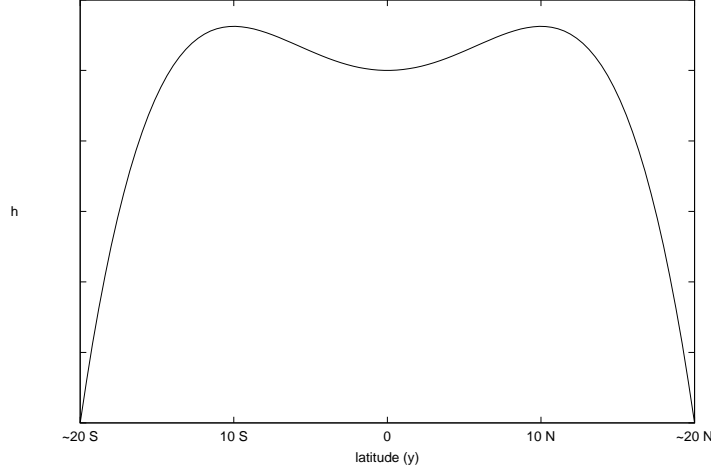


Figure 8: Layer depth as a function of latitude for a situation with non-zero zonal velocity at the equator

where the two terms on the right hand side represent the upper radiative cooling of the troposphere by long wave radiation (which is assumed to be proportional to the thickness of the layer, with a relaxation time  $\tau$ ) and the incoming source of heat  $Q(y)$  (a known function). Integrating over the whole extension of the Hadley cell, we obtain

$$\int_{-y_{max}}^{y_{max}} \partial_y(Vh)dy = 0 = \int_{-y_{max}}^{y_{max}} \left( -\frac{h}{\tau} + Q \right) dy, \quad (9)$$

on using the boundary conditions  $V(y_{max}) = V(-y_{max}) = 0$ . This constraint determines the size of the cell ( $y_{max}$ ) or, equivalently, the layer depth (i.e. temperature) at the equator,  $h_{eq}$ : we substitute our solution for  $h(y)$  into the integral to find

$$\tau \int_{-y_{max}}^{y_{max}} Q(y)dy = y_{max}h_{mid} + \frac{3}{40}\beta y_{max}^5 + \frac{1}{6}\beta U_{eq}y_{max}^3 \quad (10)$$

(an implicit equation for  $y_{max}$ ).

Although this simple model can produce a reasonable latitudinal temperature profile, it has evident limitations, particularly as it does not give the location of the ITCZ. For that, the problem must be closed by coupling the heating distribution  $Q$  to the flow and surface characteristics.

## A diffusive energy balance model

As a second example of a one-dimensional model, we extend our discussion of the ice-albedo feedback, and consider the effect of the latitudinal structure of the ice cover and the meridional transport of heat, assumed to be given by a simple down-gradient diffusion. We adopt a local coordinate system on the earth surface, and define  $y = \sin(\varphi)$ , where  $\varphi$  is the

latitude. In this coordinate system, the steady, zonally symmetrical heat equation is

$$\frac{d}{dy} \left[ (1 - y^2) D \frac{dT}{dy} \right] = OLR(T) - L_{\odot} [1 - \alpha(y)] F(y), \quad (11)$$

where  $D$  is the diffusivity, and the two terms on the right-hand side represent, respectively, the loss of energy through outgoing long wave radiation and the solar forcing. The forcing depends on the solar constant  $L_{\odot} = 1370 \text{ W m}^{-2}$ , the albedo,  $\alpha(y)$ , and the flux factor,  $F(y)$ . As a further simplification we use the linearized version of the OLR in the form,

$$OLR(T) = B(T - T^*) = BT', \quad (12)$$

where  $T' = T - T^*$  is the deviation from the reference mean temperature,  $T^*$ . The response of the system to a perturbation from the equilibrium state is thus given by

$$\frac{d}{dy} \left[ (1 - y^2) \frac{dT'}{dy} \right] = \frac{B}{D} T' - \frac{L_0}{D} (1 - \alpha) F. \quad (13)$$

As boundary conditions, we take  $T_y = 0$  at the equator,  $y = 0$ , which enforces symmetry between the two hemispheres, and insist that  $T$  be regular at the pole,  $y = 1$ .

We may exploit Green's function to write the solution to this equation in the form,

$$T(y) = -\frac{L_0}{D} \int_0^1 G(y, y') [1 - \alpha(y')] F(y') dy', \quad (14)$$

where the Green function involves the Legendre functions  $P_{\nu}(y)$  and  $Q_{\nu}(y)$  with  $\nu^2 + \nu + B/D = 0$ . However, for practical purposes, it is also straightforward to solve the differential equation numerically.

A complication in this equation is that the albedo is not simply a function of latitude, but also should depend on temperature. Nevertheless, for some simple models, we may still find the solution in the following way: consider the simple model for the albedo in which

$$\alpha = \begin{cases} \alpha_o & y < y_i \\ \alpha_i & y \geq y_i \end{cases}, \quad (15)$$

where  $\alpha_i$  is the (constant) albedo of ice,  $\alpha_o$  characterizes the albedo of unfrozen land and sea, and  $y_i$  is the latitudinal position of the edge of the ice cover (the ice margin). Then,

$$T_i = T(y_i) = -\frac{L_0}{D} \int_0^{y_i} G(y, y') (1 - \alpha_o) F(y') dy' - \frac{L_0}{D} \int_{y_i}^1 G(y, y') (1 - \alpha_i) F(y') dy'. \quad (16)$$

For consistency,  $T_i$  should be the temperature at which the ice cover first forms (273 degrees Kelvin), and so (16) determines  $y_i$  implicitly. From a practical perspective, we solve either (16) or the differential equation for given  $y_i$ , determine  $T_i$ , and then adjust  $y_i$  in order to bring  $T_i$  to the required value (such as by Newton iteration). Some sample computations are shown in figure 9. At  $y_i = 0$ , we find snowball Earth solutions (worlds with complete ice cover) provided  $T_i < 273$ . There are also solutions for ice-free worlds with  $y_i = 1$  if  $T_i > 273$ . In between, and depending on the diffusivity, there are solutions for partially

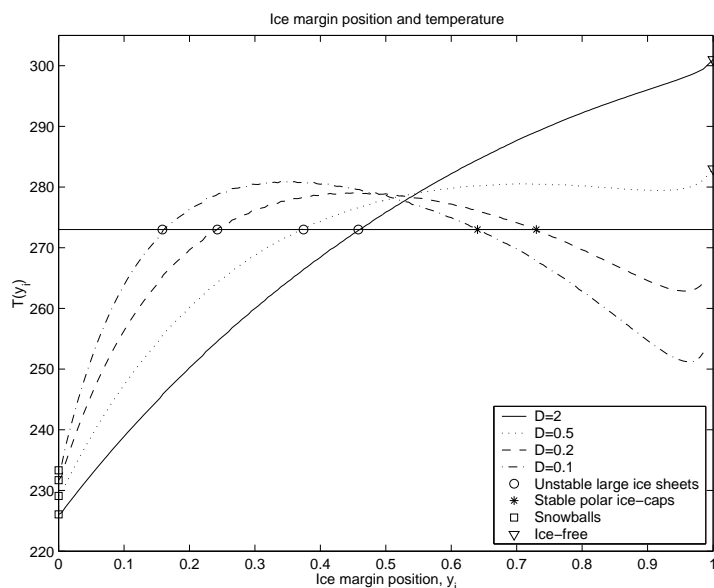


Figure 9: Ice margin position against temperature.

ice-covered worlds ( $0 < y_i < 1$  and  $T_i = 273$ ), of which one is prone to the large ice-sheet instability, and the other is a stable solution with a polar ice-cap.

Note that a natural lengthscale for the temperature variation is  $\sqrt{D/B}$ . In the limit that this scale is large, the temperature field has weak variations and we recover the zero-dimensional model described in lecture 6. Also, we need not strictly use the linearization of the OLR curve; in some problems (like greenhouse runaway), it is necessary to incorporate a nonlinear OLR curve. The numerical solution of the differential equation is no harder and proceeds in the same fashion.

Finally, we might also reinstate the time rate of change of  $T$  into the heat equation (a term like  $M\partial T/\partial t$ , where  $M$  is the “thermal mass”), in which case we could further explore the temporal rearrangements of temperature and ice cover with latitude during climate changes. This is the basis of the celebrated Sellers model (and the related Budyko model), often used by climate dynamicists.

*Notes by Lianke te Raa and Chiara Toniolo*